Journal of Mines, Metals and Fuels, *73(9): 2997-3012; 2025. DOI: 10.18311/jmmf/2025/49538*

Print ISSN : 0022-2755

Journal of Mines, Metals and Fuels

Contents available at: *www.informaticsjournals.co.in/index.php/jmmf*

Slip Casting of Alumina: Optimizing Rheological and Processing Parameters for High-Density Ceramics

Amit Kumar[1]* and Saroj Kumar Sarangi[1, 2]

[1]*Department of Mechanical Engineering, National Institute of Technology, Patna - 800005, Bihar, India; amitkumarresearchwork@gmail.com*

[2]*National Institute of Technology, Jamshedpur - 831014, Jharkhand, India*

Abstract

Slip casting is a well-established technique for shaping traditional ceramics, offering high green density, low shrinkage, and effective densification. However, its application in engineering ceramics, particularly alumina, remains limited due to the material's processing sensitivity and performance demands. This study presents a novel approach by adapting slip casting- typically not used for advanced ceramics- to produce high-density alumina bodies, positioning it as a cost-effective and geometrically versatile alternative to conventional methods such as hot pressing. The research systematically optimizes critical rheological and processing parameters including pH, solid loading, deflocculation, and viscosity. Through precise control of slurry behavior, dense and homogeneous alumina ceramics with hardness values reaching up to 1640 Vickers Pyramid number (HV) were achieved. This work demonstrates that, with appropriate parameter tuning, slip casting can be a viable route for engineering applications of alumina, expanding the potential of this low-cost processing technique. Additionally, the study identifies the detrimental role of iron inclusions, highlighting areas for further refinement in processing quality.

Major Findings: *The study highlights the critical role of advanced ceramic materials in high-temperature and structural applications due to their exceptional thermal stability, mechanical strength, and corrosion resistance. It identifies key processing techniques such as sintering, coating methods, and the integration of nanomaterials that enhance ceramic performance. The review also emphasizes the growing importance of ceramic composites and surface engineering in expanding industrial applications.*

Keywords: *Alumina Ceramics, Material Characterization, Mechanical Properties, Rheological Optimization, Slip Casting*

1.0 Introduction

Ceramics, defined as inorganic compounds formed by the chemical combination of metals and non-metals, have been extensively studied for their diverse industrial applications. Traditional ceramics, such as clays and white wares, have been used for centuries, while modern advancements have led to the development of structural and electronic ceramics with superior mechanical, thermal, and electrical properties[1,2]. These materials are widely utilized in aerospace, automotive, biomedical, and energy sectors due to their ability to withstand high temperatures, exhibit excellent wear resistance, and offer good chemical stability[3]. Structural ceramics, including alumina (Al_2O_3), silicon nitride (Si_3N_4), and zirconia (ZrO_2), have gained prominence for their superior hardness and resistance to extreme conditions. Among these, alumina stands out due to its high-temperature stability, corrosion resistance, and mechanical strength, making it a key material for applications such as cutting tools, wear-resistant coatings, and high-temperature components[4]. However, the fabrication of dense alumina

**Author for correspondence*

components remains a challenge, as traditional methods like solid-state sintering require high temperatures and extended processing times, often leading to grain coarsening and residual porosity[5].

To overcome these limitations, various processing techniques have been explored, including hot pressing, pressure-assisted sintering, and liquid-phase sintering. Hot pressing can achieve high densities but is limited by high costs and geometric constraints[6]. Alternatively, slip casting, a widely used technique in traditional ceramics, has emerged as a promising method for shaping complex alumina components while maintaining high green densities and minimizing shrinkage[7]. Recent studies have highlighted the potential of slip casting followed by sintering to produce alumina components with tailored microstructures and enhanced mechanical p roperties[8].

The optimization of slip casting parameters, such as pH, viscosity, dispersant concentration, and solid loading, plays a crucial role in achieving dense and homogeneous alumina bodies[9]. This study aims to systematically investigate the rheological behavior of alumina slips and optimize key processing parameters to enhance the densification and mechanical performance of slip-cast alumina. By addressing these factors, slip casting can be positioned as a viable and cost-effective alternative to conventional alumina fabrication techniques.

1.1 Importance of Structural Ceramics in High-temperature and Wear-resistant Applications

Structural ceramics have garnered significant attention in high-temperature and wear-resistant applications due to their exceptional mechanical, thermal, and chemical properties. Compared to metals and polymers, ceramics exhibit superior hardness, high-temperature stability, excellent corrosion resistance, and low density, making them suitable for extreme operating conditions[10]. These advantages have led to their widespread use in industries such as aerospace, automotive, energy, and biomedical engineering[11].

The ability of structural ceramics to maintain their mechanical integrity at elevated temperatures has made them indispensable in high-performance engineering applications. Alumina (Al_2O_3), silicon carbide (SiC), and silicon nitride (Si_3N_4) are commonly used in environments exceeding 1000° C, where metals typically experience oxidation and mechanical degradation[12]. Silicon carbide and silicon nitride, in particular, are widely utilized in gas turbines, heat exchangers, and aerospace components due to their excellent thermal shock resistance and low thermal expansion[13].

Alumina, one of the most widely used structural ceramics, is preferred for high-temperature applications because of its high melting point (~2050° C), chemical inertness, and good thermal insulation properties[14]. It is extensively employed in furnace linings, cutting tools, and wear-resistant coatings, where stability under extreme heat is crucial[15]. However, processing challenges, such as achieving high density and controlling grain growth, remain key research areas[16].

Structural ceramics are also highly valued for their wear resistance, which is essential in applications involving friction, impact, and abrasive environments. Alumina, zirconia (ZrO_2), and Tungsten Carbide (WC) are widely used in cutting tools, bearings, biomedical implants, and protective coatings due to their high hardness and low wear rates[17]. In coal crushing and mining industries, alumina and zirconia ceramics are preferred for wear liners and grinding media, significantly extending service life compared to conventional materials[18].

The wear resistance of ceramics is largely attributed to their strong covalent or ionic bonding, which provides high hardness and prevents plastic deformation[19]. However, their brittleness can be a limitation in impact-prone applications. Recent advancements in composite ceramics and toughened ceramic systems, such as Zirconia-Toughened Alumina (ZTA) and silicon nitride composites, have improved fracture toughness while maintaining wear resistance[20].

Given these advantages, optimizing the fabrication processes of structural ceramics, particularly alumina, is essential for maximizing their performance. Slip casting, as an alternative to conventional fabrication methods, offers the flexibility to produce complex-shaped alumina components while maintaining high density and minimizing porosity[21]. This study aims to enhance the slip casting process for alumina by optimizing critical parameters such as viscosity, pH, and dispersant concentration to achieve superior mechanical

properties for high-temperature and wear-resistant applications.

1.2 Limitations of Traditional Fabrication Methods (Hot Pressing, Solid-State Sintering)

The fabrication of high-performance structural ceramics such as alumina, silicon nitride, and zirconia relies on various processing techniques to achieve high density, mechanical strength, and wear resistance. Traditional methods, including hot pressing and solid-state sintering, have been widely used for manufacturing dense ceramic components. However, both techniques have inherent limitations that restrict their applicability, particularly in cost-sensitive and geometrically complex applications[22].

1.2.1 Hot Pressing

Hot pressing involves applying high pressure and temperature simultaneously to enhance densification and minimize porosity in ceramics. While this method can achieve near-theoretical density and improved mechanical properties, it has several drawbacks:

- Requires specialized high-pressure furnaces and expensive tooling, making it unsuitable for large-scale or cost-sensitive applications[23].
- Energy-intensive due to prolonged exposure to high temperatures and pressures[24].
- Hot pressing is primarily suitable for simple shapes, as complex geometries cannot be easily formed under uniform pressure conditions[25].
- Post-processing (*e.g.*, machining or grinding) is often required to achieve intricate designs, adding to costs and material wastage.
- The applied pressure can cause abnormal grain growth, which may reduce the mechanical performance of the final component[26].
- Residual stresses can develop during cooling, affecting fracture toughness and thermal shock resistance[27].

1.2.2 Solid-state Sintering

Solid-state sintering is another widely used method where ceramic powders are densified by applying heat below their melting point, facilitating atomic diffusion and particle bonding. Despite its effectiveness, it also has notable limitations:

- Achieving full densification without pressure is challenging, often resulting in residual porosity that weakens mechanical properties[28].
- High sintering temperatures (>1600° C for alumina) are required, increasing energy consumption and production costs[29].
- Extended sintering durations (several hours to days) are needed to allow sufficient diffusion for densification, making the process inefficient for large-scale manufacturing[30].
- Grain coarsening occurs at high temperatures, negatively affecting strength, hardness, and wear resistance[31].
- Additives are often required to promote densification, which may alter the ceramic's chemical and mechanical properties[32].
- Significant shrinkage (~15-25%) occurs during sintering, leading to dimensional inaccuracy and potential warping, particularly for large or complex parts[33].

1.3 Need for Alternative Fabrication Methods

Given these limitations, alternative fabrication techniques such as slip casting have gained interest for producing complex-shaped ceramics with high green densities and lower production costs. Slip casting allows for better control over particle distribution, reduced shrinkage, and flexibility in shaping without the geometric constraints of hot pressing or the prolonged processing times of solid-state sintering[34]. This study explores the optimization of slip casting parameters for alumina to overcome these challenges and enhance its mechanical performance.

Given the limitations of traditional ceramic fabrication techniques such as hot pressing and solid-state sintering, alternative methods are being explored to produce high-density, complex-shaped ceramics more cost-effectively. Among these, slip casting has emerged as a promising technique for fabricating structural ceramics, particularly alumina, due to its ability to produce intricate geometries while maintaining high green densities and minimizing shrinkage[35].

Slip casting is a well-established forming technique traditionally used for manufacturing clay-based ceramics

and white wares. It involves preparing a stable ceramic suspension (slip) by dispersing fine ceramic powders in a liquid medium, typically water, with the aid of dispersants and deflocculants to control viscosity[36]. The slip is then poured into a porous mold, usually made of plaster, which absorbs the liquid, allowing the ceramic particles to consolidate along the mold walls. Once a sufficient thickness is achieved, the excess slip is drained, and the green body is dried before undergoing sintering to achieve full densification[37]. There are several advantages of slip casting method over traditional methods; some of them are listed below;

- Unlike hot pressing, which is limited to simple geometries, slip casting allows for the fabrication of intricate and large ceramic components without requiring expensive machining[38].
- Slip casting does not require high pressures or specialized equipment, making it more economical than pressure-assisted methods like hot pressing[39].
- Energy consumption is reduced as sintering temperatures can be optimized with proper particle packing and binder selection[40].
- The slip preparation process enables precise control over particle distribution, viscosity, and solid loading, reducing porosity and improving final density[41].
- Proper dispersion techniques can help mitigate defects such as agglomeration and in homogeneity, leading to improved mechanical properties[42].
- Slip casting is well-suited for large-scale manufacturing, allowing for the efficient production of multiple components using reusable molds[43].

1.4 Challenges and Optimization Requirements

Despite its advantages, slip casting requires careful optimization of several parameters, including pH, viscosity, solid loading, and deflocculant concentration, to achieve high-density and defect-free alumina components[44]. Uncontrolled flocculation or poor slip stability can lead to particle settling, uneven drying, and increased porosity; affecting the mechanical performance of the final product[45,46]. This study aims to systematically investigate the key processing parameters governing slip casting for alumina fabrication. By optimizing slip rheology, green body formation, and sintering conditions, the research seeks to develop a more efficient and reliable method for producing high-performance alumina components suitable for high-temperature and wear-resistant applications[47-49].

The literature highlights that structural ceramics, particularly alumina (Al_2O_3), offer exceptional high-temperature stability, wear resistance, and corrosion resistance, making them ideal for applications in aerospace, automotive, and industrial sectors. However, traditional fabrication methods like hot pressing and solid-state sintering face significant challenges, including high costs, geometric limitations, prolonged processing times, and residual porosity. Slip casting has emerged as a promising alternative, enabling complex shaping with high green densities while maintaining cost-effectiveness and scalability. Studies emphasize that optimizing slip casting parameters such as pH, viscosity, dispersant concentration, and solid loading is crucial for achieving dense, defect-free alumina bodies. Proper deflocculation and slip stability prevent processing defects like warping and porosity, leading to improved mechanical properties, including hardness up to 1640 Vickers Pyramid number (HV). Despite these advantages, iron inclusions during processing can limit the final strength, necessitating careful material selection and process control. Future research should focus on advanced sintering techniques, novel dispersants, and composite formulations like Zirconia-Toughened Alumina (ZTA) to further enhance mechanical performance, fracture toughness, and wear resistance in slip-cast ceramics.

In this article, the authors have systematically investigated the optimization of slip casting parameters to enhance the densification and mechanical properties of alumina ceramics. They have focused on key processing factors such as pH, viscosity, dispersant concentration, and solid loading to achieve high-density, defect-free alumina bodies. A detailed rheological study of alumina slip was conducted to ensure proper fluidization and stability, preventing issues like particle agglomeration and inhomogeneous drying. The influence of these parameters on the final microstructure and mechanical performance was analyzed, with particular emphasis on minimizing porosity and achieving high hardness values, reaching up to 1640 Vickers Pyramid number (HV) after sintering. Additionally, the study highlights the challenges

Table 1. Composition of selected compounds

Compound composition, wt%					
Compound	**Al_2O_3**	**ZY8**	**ZrO_2(m)**	**SiC**	**TiO2**
	µm	µm	µm	µm	µm
A	100.0	-	-	-	-
A1	80.0	-	20.0	-	-
A2	80.0	20.0	-	-	-
B1	97.0	-	-	3.0	-
B2	95.0	-	-	-	5.0

posed by iron inclusions in processing and their impact on strength. Through this work, the authors demonstrate that slip casting, when carefully optimized, presents a viable and cost-effective alternative to traditional fabrication methods for producing high-performance alumina ceramics.

2.0 Experimental Procedure

Slip casting has been used in experiments to create ceramics, composites, and soft molds made of Polydimethylsiloxane (PDMS). Characterization procedures, including property measurements at various processing stages and pertinent analytical techniques for assessing material performance, are also included in the research.

2.1 Raw Materials

This study employed a variety of alumina matrix composites, including pure alumina α-Al_2O_3 (A), alumina-20 weight percent zirconia composite with unstabilized ZrO_2 (A1), alumina-20 weight percent zirconia composite with 8 weight percent Y_2O_3 partially stabilized ZrO2 (Y-PSZ) (A2), alumina-3 weight percent silicon carbide (B1), and alumina-5 weight percent titania (B2). α-Al_2O_3 99.8% type A16SG, a high-purity alumina powder with an average particle size of less than 0.5 µm, was utilized. Alumina-based composites were used in the trials, along with several kinds of ceramic composites. Table 1 displays the original compositions of the compounds chosen for testing.

Commercial polymer dispersants were used to deflocculate the powders prior to slip casting, Dolapix CE 64. Dolapix CE 64 is an aqueous solution of ammonium salt of a polyelectrolyte. Room temperature properties of the dispersants are given in Table 2.

Table 2. Room temperature properties of Dolapix CE 64

Physical Properties	Dolapix CE 64
Active matter (wt %)	70
Density (g/cm3)	1.10
pH	7.0
Solubility characteristics	Completely soluble in water systems

2.2 Processing of Ceramic Slurry

To find the ideal conditions for stabilizing slurries with high solids content (70 wt.), slurries with solids contents of 40, 50, 60, and 70 wt. % were created. The dispersant was added to slurry with a certain solids concentration, and the slurries were then aged for 16 hours while being stirred mechanically. A rotating spindle viscometer (Brookfield RVT DV-II) was used to measure the viscosity of the slurry just after aging. At every shear rate (rotational speed) where a reading of the viscosity values could be achieved, sets of measurements were made using a particular spindle. By monitoring the pace at which the par zticles settled within glass test tubes, the stability of each as-prepared slurry sample was assessed.

Slip casting was then employed to create rectangular specimens using the slurries. For two hours, each mold was maintained in this condition. Until the whole mold was filled with the green cast specimen and a solid cast was produced, the quantity of water that the mold walls absorbed was gradually replenished with fresh slurry.

The specimens were cast, dried for six hours at 110° C, and then burned at 1600° C. The Vickers hardness measurement (Tukon 2100 B), microstructure (scanning electron microscopy, ZEISS), and density (Archimedes technique) were all used to assess the burned specimens.

2.3 Flow Chart for the Preparation of Slurry for the Slip Casting

A slurry is formulated utilizing alumina (70 wt.%) and YSZ (20 wt.%) as raw materials, along with distilled water, concentrated sulfuric acid, and ammonium polymethylacrylic acid at 0.5% of solid loading (Dolapix CE 64), along with a 5 wt.% solution of Polyacrylic Acid (PAA). The mixture is magnetically agitated for uniform blending then milled at 1000 rpm for 24 hours. Figure 1 illustrates the comprehensive slurry preparation process using a flow chart.

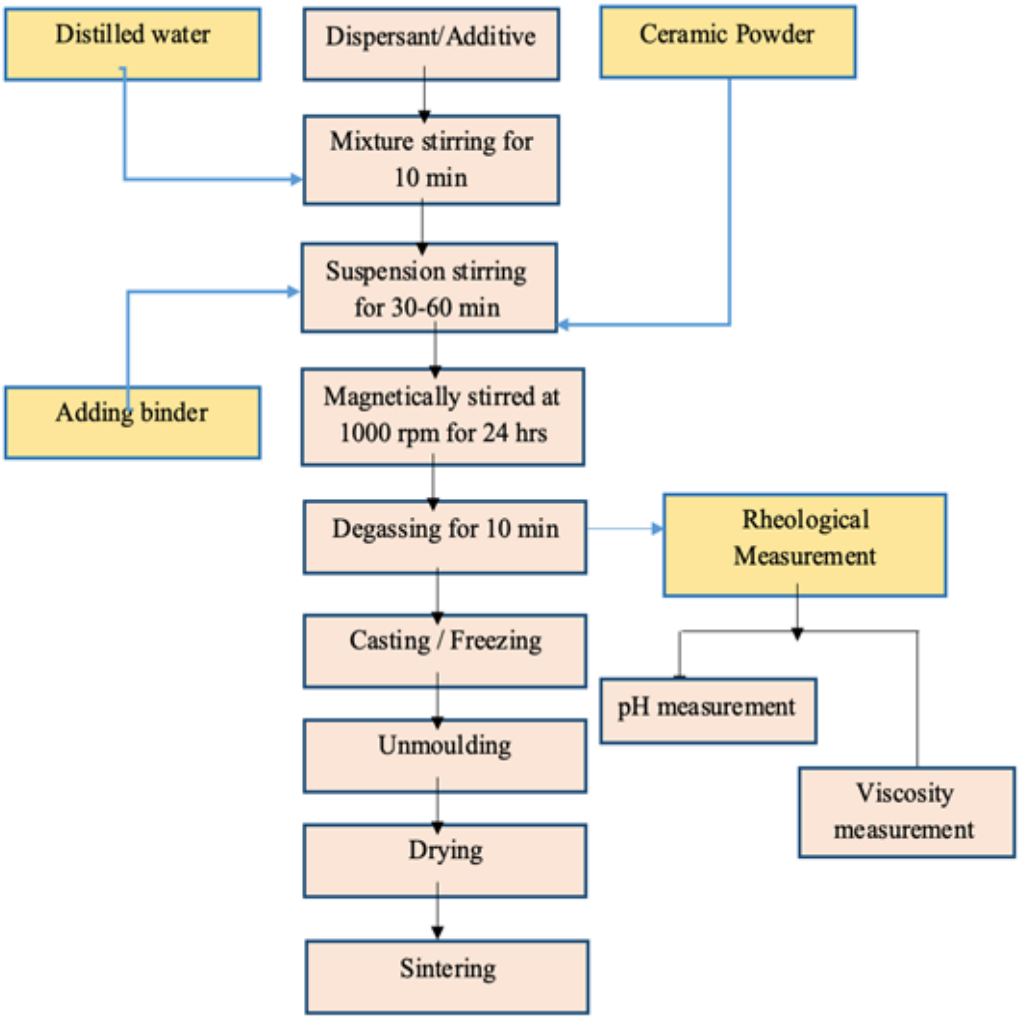


Figure 1. Flowchart for whole process of preparation of slurry.

2.4 Viscosity Measurement

The viscosities of alumina slurries with different solid loadings and pH levels were assessed using the viscosity measuring device depicted in Figure 2. The viscosity of the slurry was measured using a rotating spindle viscometer (Brookfield RVT DV-II). Measurements using a particular spindle were conducted at all shear rates (rotational speeds) where viscosity values could be recorded.



Figure 2. Image of Brookfield viscometer used for measuring viscosity of slurry.

2.5 Mould Preparation

Commercial grade potters plaster was used for making moulds. For every 100g of plaster, 80 ml of water were added, as mould made with this plaster: Water ratio have been shown to exhibit maximum water removal capacity. The water was added to the plaster and allowed to stand for 1 minute. Using a smaller submerged propeller blade the mixture was rapidly stirred for 3 minute and then quickly poured in PDMS mould, previously greased with Vaseline. Blocks of plaster were cast with approximate dimensions 10cm x 5cm x 7cm when dry. These were then heated in oven to remove water completely. The mould preparation and sample were casted as shown in Figure 3. Using this type of mould, samples in the shape of bars were cast having dimensions 9.7cm x 4.8cm x 5 cm.

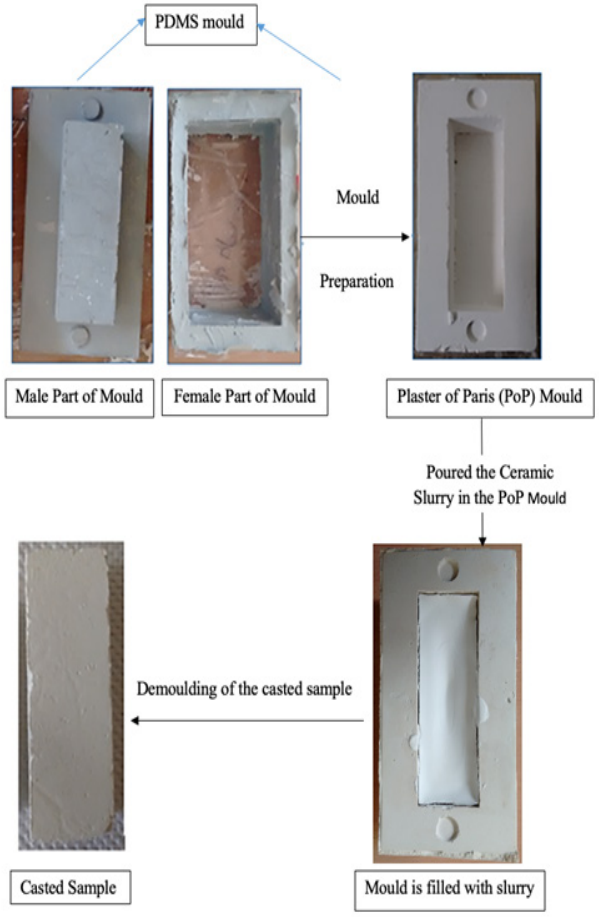


Figure 3. Step for preparing the plaster of paris mould and casting the sample.

2.6 Drying and Sintering

The green samples which were taken out from the mould were placed in the air for drying for 1 day completely. The sample after drying in air heated in oven for 5-6 hrs at a temperature of 120° C to give some strength in the green stage. After the heating of the samples in oven they were placed in the furnace at a temperature of 145° C. The heating rate, holding and cooling rate is shown in the Figure 4.

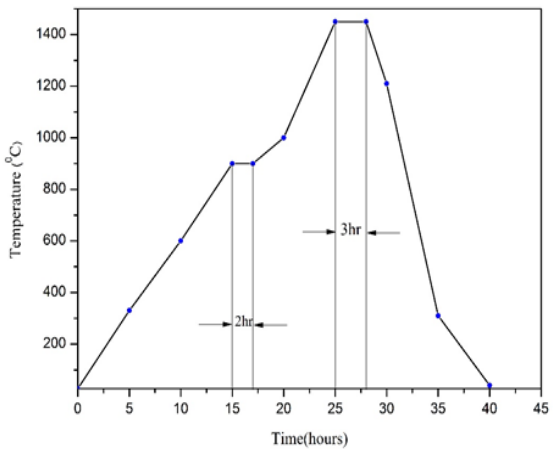


Figure 4. Schematic diagram of sintering regime of all green samples.

3.0 Results and Discussion

3.1 Dispersion of Suspensions

Suspensions- a mixture of solid particles in a liquid- are particularly interesting in the production of ceramics. They are being utilized more and more to create the green body by consolidating ceramic granules. Colloidal techniques can result in higher packing homogeneity in the green body, which in turn leads to better micro structural control during fire, as opposed to powder consolidation in the dry or semidry state (such as pressing in a die). Polymer molecules dissolved in a liquid make up colloidal solutions.

The dispersion of suspensions is a fundamental issue that we will address. It is obvious that if the particles are too big, gravity will cause them to sediment quickly. The force of attraction between the particles is the second crucial element. Regardless of the presence of additional interactions, there are attractive Van-der Waals forces between the particles. Particles will collide and adhere to one another if the attraction force is strong enough, which will cause flocculation or coagulation, or the rapid sedimentation of particle clusters. The methods used to stop flocculation rely on the introduction of repulsive forces, even if in theory the lowering of the attractive force can also be utilized. The fundamental methods employed are repulsion between electrostatic charges (electrostatic stabilization), repulsion between polymer molecules (steric stabilization), or a combination of the two (electrosteric stabilization). Because it regulates the packing regularity of the consolidated body, the stability of colloidal suspensions has to be fundamentally understood. While an unstable suspension can result in a loosely packed structure or, in some cases, a particulate gel with a relatively large volume, a stable colloidal suspension can be consolidated into a densely packed structure.

This chapter will go over how to prevent particle agglomeration in order to create a low viscosity solution and a homogeneous microstructure, which will provide a densely packed structure with a high density and hardness value.

3.1.1 Slip Viscosity Behaviour

Figure 5 shows the variation of viscosity with varying amounts of Dolapix CE for solid loadings. Viscosity was measured at shear rate of 100 rpm. From these graph it is apparent that for a given solid loading, viscosity decreases as the amount of Dolapix CE 64 increases, until a minimum is obtained. On further increasing, the Dolapix CE 64 concentration, viscosity increases again.

Dolapix CE 64, a polyelectrolyte of Ammonium methyl methacrylate, is proprietary and the exact composition is not known. This polyelectrolyte has been used earlier and has been found to be an

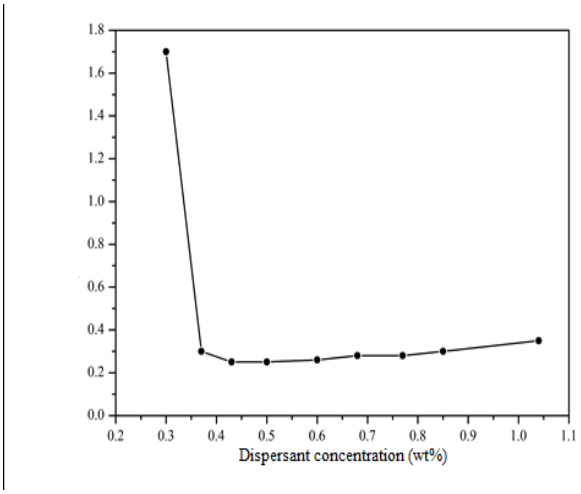


Figure 5. Viscosity versus dispersant concentration of 70 wt.% alumina slurry.

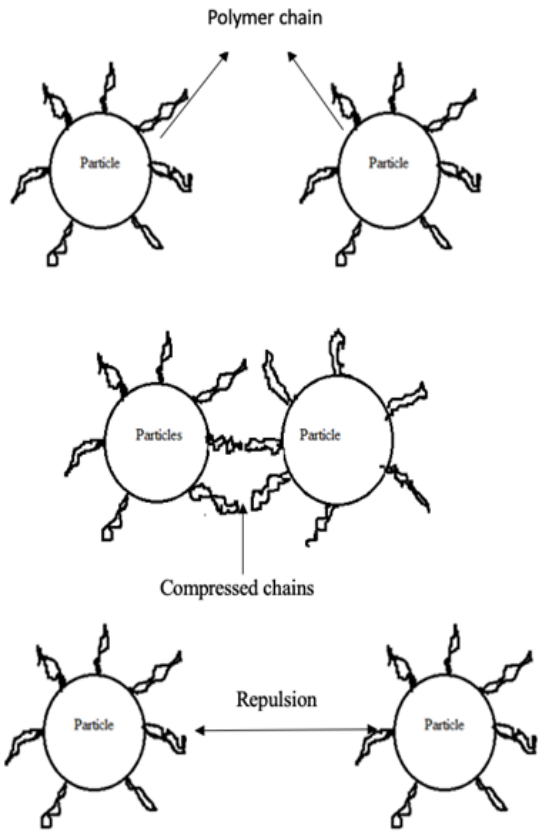


Figure 6. **(a)** Two particles with polymer chains approaching one another **(b)** Compressed chains at closest approach **(c)** Repulsion due to force exerted by the compressed chains.

effective dispersant for ceramic slips. It is however, an ammonium salt of Methyl methacrylate and dissociates in water to give NH_4^+ ions and methacrylate poly-ions. Dolapix CE 64 being used, the slurry is being stabilized by both electrostatic interactions and polymer adsorption.

When Dolapix CE 64 is added to a slip the methacrylate poly-ions tend to be adsorbed on the surface particles. This diffuse layer gives the particles a negative charge. The excess of the positive ions (NH_4^+ and H^+) in the solution then surround the diffuse layer due to electrostatic attraction. The particles being negatively charged, repel each other and the system deflocculates. It should be noted that repulsive forces can also arise due to non-ionic polymer adsorption on the particle surface. Absorption of non-ionic polymers on the particle surface can result in both attractive and repulsive forces. Attractive forces can arise from polymer bridging when there is a direct link between two particles through a polymer bridge. Repulsive forces arise in 2 ways when 2 polymer adsorbed particles approach each other. As the particles come close to each other, the polymer concentration increases more in the gap between the particles than in the general solution resulting in osmotic pressure difference between the gap and the solution. This decreases the entropy of the system, and in turn increases the Gibbs free energy. This increase in energy causes repulsion between particles. The polymer chains can also interpenetrate and compress each other which results in forcing the particles apart. This can be visualised by compressing a simple circular spring as shown in Figure 6.

Kalin *et al.* have shown that a low viscosity of a slip is associated with a high zeta potential and vice versa. Increasing the amount of Dolapix CE 64 can have two opposing effects: (1) Increase in zeta potential (low viscosity) due to increased surface charge, and (2) Decrease in zeta potential (high viscosity) due to compressed diffuse layer. From the discussion so far an optimum amount of Dolapix CE 64 must be added to the slurry to produce a fully deflocculated system.

3.1.2 Viscosity vs pH

It is well known that the surface charges of particles in a polar media, such as water, affect whether they

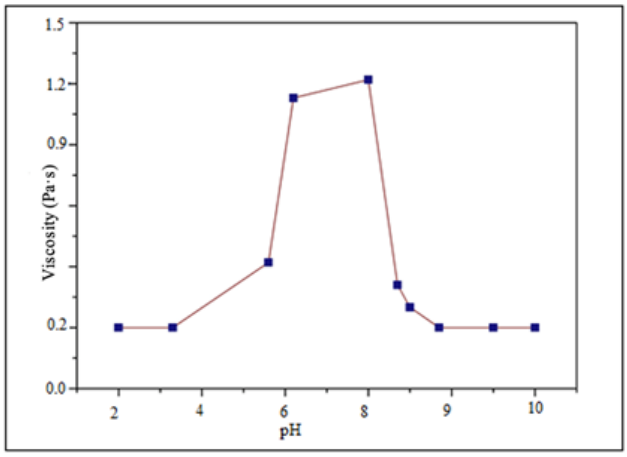


Figure 7. The apparent viscosity vs pH values for 70 wt% at 100 rpm (weight percent of total amount of alumina and water in the slurry) slurries.

aggregate or disperse. Depending on their polarity and the amount of surface charges they have accumulated, the particles either flocculate or deflocculate in response to pH variations. Figure 7 illustrates how pH affects the way alumina particles disperse in deionized water.

As the slurry's solid concentration rises, the viscosity in Figure 7 continues to rise. When the solid content is less than 50 weight percent, the viscosity increases gradually as the solid content rises, but when the solid content rises over 50 weight percent, it increases quickly. When the solids concentration is 50 weight percent, the viscosity reaches around 50 mPa.s. In general, a slip casting technique needs concentrated ceramic slurries that are less viscous and evenly distributed. Therefore, 70 weight percent was the maximum solid loading allowed for slip casting in this program. Figure 7 shows the viscosity of 70 weight percent alumina slips as a function of pH at a shear velocity of 100 s^{-1}. Lower viscosities are seen between pH values of 2 and 4 and between pH values of 9 and 10. This demonstrates how evenly distributed the granules are over this pH range. A flocculated suspension is characterized by greater viscosities in the pH range of 6 to 8.5.

3.1.3 Viscosity vs Solid Loadings

Shear rates also affect viscosities for a given solid loading.

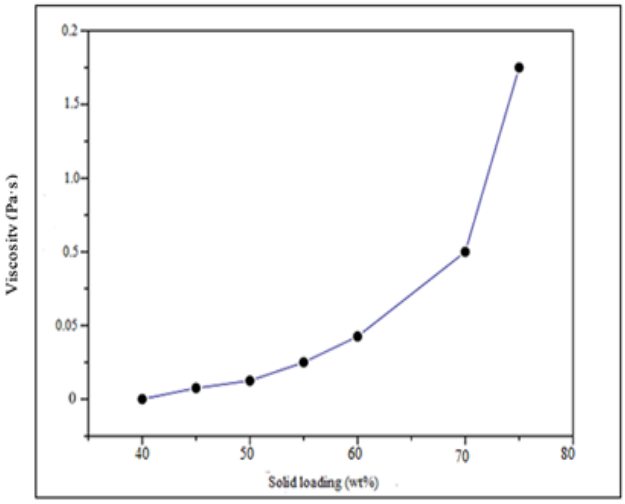


Figure 8. Viscosity versus solids content for the slurries near pH 6 at the 100 rpm.

These slips show thixotropy and are not Newtonian. In thixotropy, shear action breaks apart the agglomerates, which then reunite when the shear rate is decreased. Figure 8 shows how the viscosity increases as the slurry's solid concentration rises. When the solid content is less than 50 weight percent, the viscosity increases gradually as the solid content rises, but when the solid content rises over 50 weight percent, it increases quickly. When the solids concentration is 50 weight percent, the viscosity reaches around 50 mPa.s. In general, a slip casting technique needs concentrated ceramic slurries that are less viscous and evenly distributed. Therefore, 70 weight percent was the maximum solid loading allowed for slip casting in this program.

3.2 X-Ray Diffraction (XRD) Analysis

The Rigaku X-Ray Diffractometer was used to perform X-Ray Diffraction analysis on all samples under the same circumstances using CuKα radiation with wavelength (λ) = 1.54A0, tube voltage of 40 kV, and tube current of 30 mA.

Range of Scan: 10°-80°

Continuous Scan Mode; 50/min Speed

The complete XRD examination was conducted using these conditions. The diffraction intensity Vs 2θ plot, where θ is the Bragg's angle in degrees, is provided by the XRD spectrum.

The respective peaks in the XRD plot of alumina were matched with the standard JCPDS data and all the phases * corresponding to each of these peaks was identified. Also, in case of the YSZ-Alumina composite samples all the phases # and * corresponding to each of these peaks were identified from the standard JCPDS data.

The pure alumina samples were soaked for three hours at 1450° C before their XRD data was obtained. Additionally, XRD data of the YSZ-Alumina composite samples were obtained at the same soaking duration and temperature of 1450° C.

Here, alumina is combined with YSZ. An additional peak was discovered in the XRD plot as a result of the use of YSZ. In the XRD plot, the samples peaks were attributed to pure α-alumina and YSZ.

Figure 9, which displays the various attributes of the samples, derived from the XRD data.

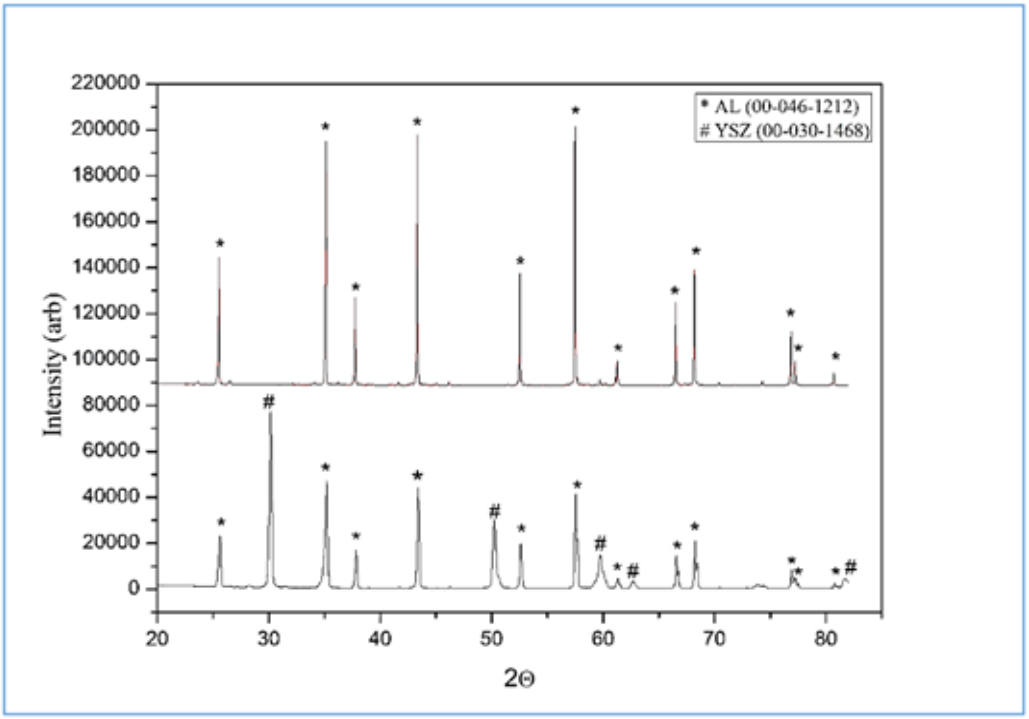


Figure 9. XRD image showing the peak of Y-PSZ and Alumina sintered at 1450° C

3.3 Particle Size Distribution

Understanding the average particle size and range of the particles present is made easier by the particle size distribution. The raw alumina powder's particle size distribution is displayed in Figures 10 (a) and (b). A mono-modal size distribution is revealed by the particle size measurement. According to the figure, the average particle size was determined to be 0.353 micron, and

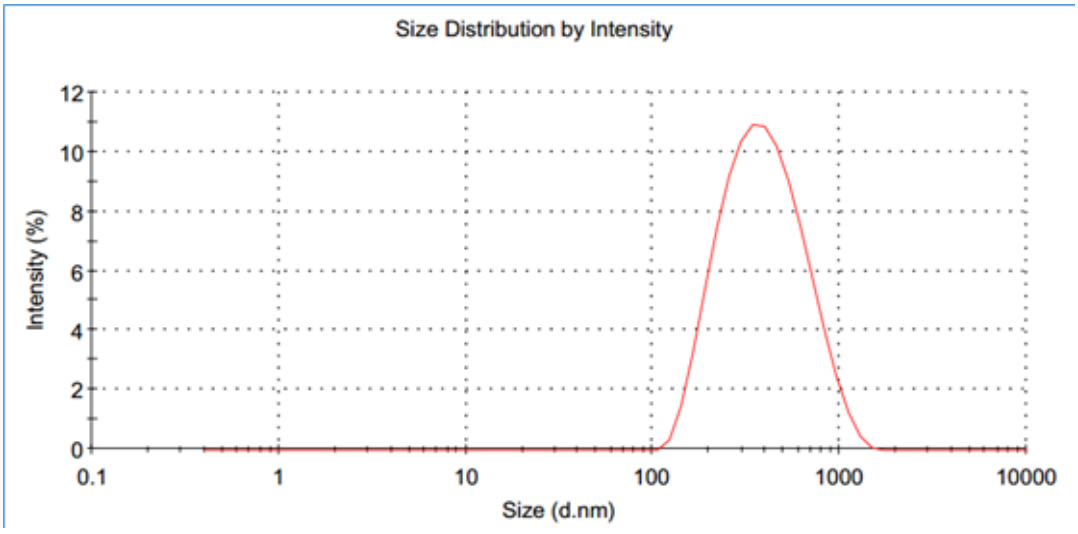


Figure 10(a). Particle size distribution with intensity % of starting powders.

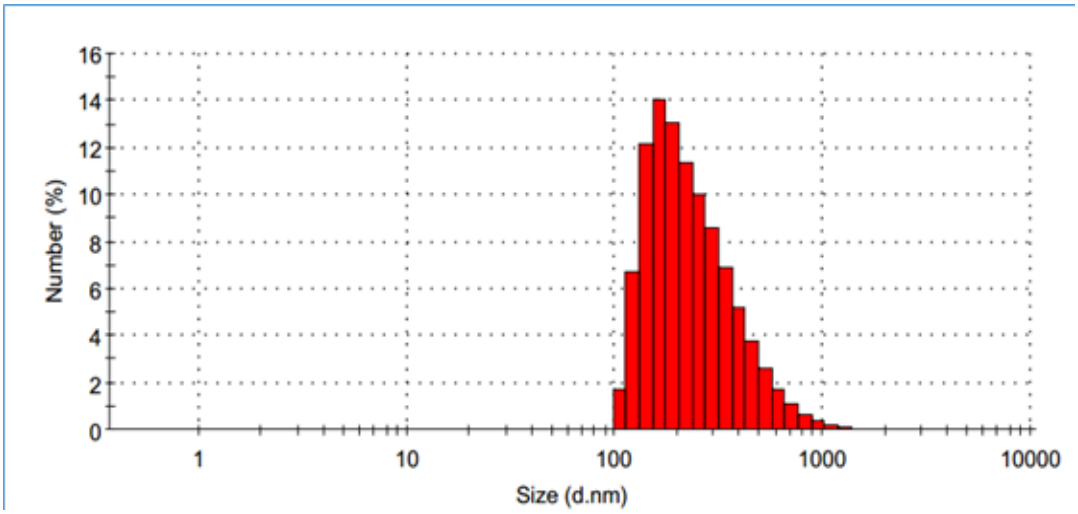


Figure 10(b). Particle size distribution with number % of starting powders.

the particle sizes ranged from 0.250 micron to 1.250 micron.

Similar findings are also displayed in the particle size distribution statistics graph (Figure 10b). As seen in Figure 10(b), the largest percentage of particles (~40%) is smaller than 1 micron.

3.4 Microscope Study (SEM)

The SEM (Scanning Electron Microscope) used for the microscopic examination of the samples has a broad depth of field, which enables a significant portion of the sample to be in focus at once and creates a picture that accurately depicts the three-dimensional sample. Numerous topographical and elemental details, such as grain size, surface roughness, porosity, particle size distributions, material homogeneity, *etc*., may be obtained using SEM.

For the SEM we use thermal etched sample. The main aim of doing SEM is to study the grain size, particle size distributions and also to study the homogeneity of the distribution of YSZ in alumina matrix. For these reasons we study the SEM of the YSZ- alumina composite powders sintered at 1450° C temperatures.

The SEM images of pure- AL and Alumina+YSZ are displayed in Figures 11 and 12. Higher magnification of the micrograph shows that the presence of YSZ reduces the alumina's particle size. The microstructure of pure alumina sintered at 1450° C with an average grain size of 1.4518 m is displayed in Figure 11. The micrograph of Alumina+YSZ sintered at 1450° C with an average grain size of 0.8908 m is displayed in Figure 12. In comparison to Figure 11, the SEM picture of Figure 12 revealed a considerable reduction in the size of the alumina grains.

SEM micrographs of Al_2O_3 and Al-doped Y-PSZ are displayed in Figures 11 and 12, respectively. Al-doped Y-PSZ particles had a different shape from Al_2O_3 particles; although Al_2O_3 and Y-PSZ particles had sharp, smooth edges, Al-doped Y-PSZ particles had round, rough ones. Due to its poor solubility, Al_2O_3 does not form a solid solution with zirconia; as a result, it exists in zirconia as

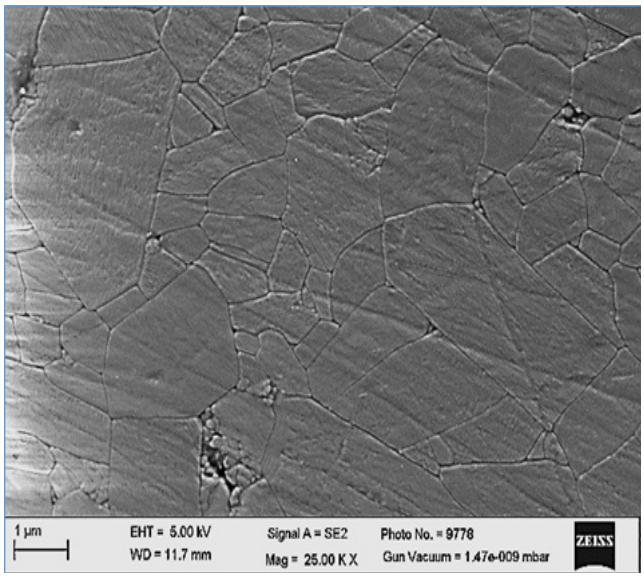


Figure 11. SEM image of thermal etched pure Alumina sintered at 1450° C.

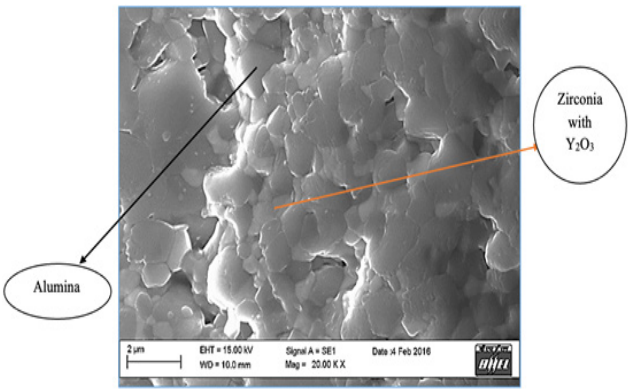


Figure 12. SEM image of thermal etched sample of Y-PSZ +Alumina sintered at 1450° C.

a separate phase, and for Al-doped Y-PSZ, a combination of ZrO_2 particles and fine Al_2O_3 particles is anticipated. The greater density and hardness of Al-doped Y-PSZ in comparison to Al_2O_3 were caused by the finer particles and the form of the particles.

The microstructure of 20 weight percent Al doped Y-PSZ sintered at 1450° C is seen in Figures 11 and 12. The micrograph (4.8) displays a fine-grained Al_2O_3 matrix (the darker phase) with uniformly dispersed ZrO_2 grains (the brighter phase). The ZrO_2 particles inhabited the intergranular borders and frequently the triple points between 1450° C grains because they prevented the Al_2O_3 grains from growing during the last sintering stage (1450 ^{0}C) (Figure 12). As a result, the alumina was pinned and grain development was inhibited. As the ZrO_2 concentration in the composites rose, so did this pinning effect; more ZrO_2 particles could pin the Al_2O_3 grain borders, which would reduce the development of Al_2O_3 grains. The fast grain development for Al_2O_3 at 1400° C was 1.7 times larger than the grain diameter measured for the composites containing 20 weight percent Al doped Y-PSZ.

4.5 Hardness and Density Measurement

The hardness measurement was done using a Vickers micro hardness tester at 30 kg load and four measurements were taken for each sample to reduce the errors and obtained values are cited in the Table 3.

Table 4 displays the impact of various ceramics on Al_2O_3's hardness. As a result, the sample's hardness was determined to be both higher and lower than the undoped samples. This outcome can be seen at a sintering temperature of 1450° C, where the measured hardness for the 20 weight percent Y-PSZ doped sample was 1604 Hv, whereas the undoped alumina reached 1480 Hv. Additionally, compared to all other samples sintered at the same temperature, it appears to have a greater hardness.

4.5.1 Density Measurement

Porosity % = (Theoretical density - Experimental density) / Theoretical density

Table 3. Micro hardness values for the composite sintered at 1450° C

Sample	1	2	3	4	Average Hardness (Hv)
A	1515	1472	1507	1426	1480
A1	1100	1109	1083	1047	1084.75
A2	1576	1640	1610	1590	1604
B1	650	720	693	685	684
B2	933	1005	957	978	968.25

Table 4. Table comparing the % porosity of composite

Composites	Theoretical density	Experimental density	Porosity %
A	3.850	3.303	14.274
A1	4.210	3.114	26.033
A2	4.30	3.447	19.837
B1	3.812	2.563	32.764
B2	3.868	3.113	20.036

The theoretical density is measured by the give equation 5.1 known as the rules of mixture

$$\rho = \frac{V_a \rho_a}{V} + \frac{V_b \rho_b}{V} \quad (5.1)$$

Where ρ is the theoretical density of the composite, V_a and V_b are volume fractions of constitutes, ρ_a and ρ_b are the density of constitutes.

The experimental density is calculated with the help of buoyancy method.

5.0 Conclusions

This study systematically investigated the slip casting of alumina by optimizing the rheological behavior of aqueous slurries. Critical parameters such as viscosity, solid loading, dispersant type and concentration, porosity, and resultant hardness were examined to enhance the performance and quality of the cast bodies. The following conclusions can be drawn:

5.1 Dispersant Concentration Effect

Increasing dispersant concentration initially reduces the viscosity of the slip at a given solid loading, reaching a minimum point. Beyond this optimum, further increase in dispersant leads to a rise in viscosity due to over-dispersion or flocculation.

5.2 Optimal Viscosity and Solid Loading

The minimum viscosity value corresponds to the optimal solid loading and serves as a key indicator for producing well-deflocculated, castable slips.

5.3 Optimal Slip Composition

Among the formulations tested, the most rheologically stable and castable slips were achieved using Dolapix CE 64 at 0.5 wt% dispersant concentration and 70 wt% solid loading, enabling efficient shaping and densification.

5.4 Microstructure-hardness Relationship

A significant reduction in hardness was observed when the average grain size of sintered Al_2O_3 exceeded approximately 1 μm, highlighting the importance of grain growth control in achieving high mechanical performance.

5.5 Effect of Y-PSZ Additions

The addition of Yttria-Partially Stabilized Zirconia (Y-PSZ) improved both hardness and densification. Hardness values in the range of 1480-1604 HV were attained at approximately 90% of the theoretical density.

Among all compositions, 20 wt% Y-PSZ added to Al_2O_3 and sintered at 1450° C yielded the highest hardness, indicating its effectiveness in enhancing the mechanical strength of the composite. In general, an increase in sintering temperature led to improved densification of alumina.

6.0 References

1. Srivastava SK, Gupta GK, Joshi TC, Pandey A, Muchhala D, Shrivastava V, *et al*. Existence of advanced ceramic materials in human life. ACVIA. 2022:1-14. https://doi.org/10.1016/B978-0-323-89952-9.00013-0
2. Kumar R, Pandey RK, Shukla SS, Gidwani B. Ceramic fillers, fibers, and acrylics. Magnetic Polymer Composites and Their Emerging Applications. 1st

Edition. CRC Press. 2024: pp. 289-313. https://doi.org/10.1201/9781003454236-15
3. Saunders SRJ, Nicholls JR. Coatings and surface treatments for high temperature oxidation resistance. Mater Sci Technol. 1989; 5(8):780-798. https://doi.org/10.1179/026708389790222843
4. Kucita P. The development of a wear resistance aluminium bronzes (Cu-Al-Fe) coating. University of Southampton Institutional Repository. 2016. http://eprints.soton.ac.uk/id/eprint/403720
5. German RM. Coarsening in sintering: Grain shape distribution, grain size distribution, and grain growth kinetics in solid-pore systems. Crit Rev Solid State Mater Sci. 2010; 35(4):263-305. https://doi.org/10.1080/10408436.2010.525197
6. Ramirez JMH, Bustamante RP, Merino CAI, Morquecho AMA. Unconventional techniques for the production of light alloys and composites. Springer. 2020. https://doi.org/10.1007/978-3-030-48122-3
7. Rice RW. Ceramic processing: An overview. AIChE J. 1990; 36(4):481-510. https://doi.org/10.1002/aic.690360402
8. Ali M, Khan DSA. Additive manufacturing of functional parts from ceramics. Addit Manuf Funct Ceram. 2023.
9. Indacochea JE, Smith JL, Litko KR, Karell EJ, Rarez AG. High-temperature oxidation and corrosion of structural materials in molten chlorides. Oxid Met. 2001; 55:1-16. https://doi.org/10.1023/A:1010333407304
10. Rahman MZ, Rahman M, Mahbub T, Ashiquzzaman M, Sagadevan S, Hoque ME. Advanced biopolymers for automobile and aviation engineering applications. J Polym Res. 2023; 30(106). https://doi.org/10.1007/s10965-023-03440-z
11. Oues AK. Protection optimization of carbon-carbon composites against air oxidation by coating with anti-oxidants. Southern Illinois University. 2017.
12. Fahrenholtz WG, Wuchina EJ, Lee WE, Zhou Y. Ultra-high temperature ceramics: Materials for extreme environment applications. John Wiley and Sons; 2014.
13. Brook RJ. Concise encyclopedia of advanced ceramic materials. Elsevier; 2012.
14. Hakimeh W. Colloidal filtration of alumina-zirconia with solid oxide additives. University of Malaya; 2012.
15. Binner J, Porter M, Baker B, Zou J, Venkatachalam V, Diaz VR, *et al*. Selection, processing, properties and applications of ultra-high temperature ceramic matrix composites, UHTCMCs: A review. Int Mater Rev. 2020; 65(7):389-444. https://doi.org/10.1080/09506608.2019.1652006
16. Yang L. Nanotechnology-enhanced orthopedic materials: Fabrications, applications and future trends. MRS Bulletin. Woodhead Publishing. 2015; 42(1):234. https://doi.org/10.1557/mrs.2016.318
17. Finch CA. Kirk-Othmer concise encyclopedia of chemical technology. Br Polym J. 1986; 18(6):400. https://doi.org/10.1002/pi.4980180615
18. Barker KC. The development of abrasive-corrosive wear resistance of steels by microstructural control; 1988.
19. Wang J, Stevens R. Zirconia-toughened alumina (ZTA) ceramics. J Mater Sci. 1989; 24:3421-3440.
20. Singh S, Das PK, Mondal DP. Advanced ceramics for versatile interdisciplinary applications. Elsevier; 2022.
21. Dobrzanski LA, Dobrzanski LB, Danikiewicz ADD. Overview of conventional technologies using the powders of metals, their alloys and ceramics in Industry 4.0 stage. J Achiev Mater Manuf Eng. 2020; 2(98):56-85. https://doi.org/10.5604/01.3001.0014.1481
22. Buchanan C, Gardner L. Metal 3D printing in construction: A review of methods, research, applications, opportunities and challenges. Eng Struct. 2019; 180:332-348. https://doi.org/10.1016/j.engstruct.2018.11.045
23. Toepfl S, Mathys A, Heinz V, Knorr D. Potential of high hydrostatic pressure and pulsed electric fields for energy efficient and environmentally friendly food processing. Food Rev Int. 2006; 22(4):405-423. https://doi.org/10.1080/87559120600865164
24. Clarke DR, Faber KT. Fracture of ceramics and glasses. J Phys Chem Solids. 1987; 48(11):1115-1157. https://doi.org/10.1016/0022-3697(87)90121-1
25. Mitomo M, Tajima Y. Sintering, properties and applications of silicon nitride and sialon ceramics. J Ceram Soc Jpn. 1991; 99(1154):1014-1025.
26. Clyne TW, Gill SC. Residual stresses in thermal spray coatings and their effect on interfacial adhesion: A review of recent work. J Therm Spray Technol. 1996; 5:401-418.
27. Oguntuyi SD, Johnson OT, Shongwe MB, Jeje SO, Rominiyi AL. The effects of sintering additives on the ceramic matrix composite of ZrO_2: Microstructure, densification, and mechanical properties- a review. Adv Appl Ceram. 2021; 120(5-8):319-335. https://doi.org/10.1080/17436753.2021.1953845
28. Binner J, Porter M, Baker B, Zou J, Venkatachalam V, Diaz VR, *et al*. Selection, processing, properties and applications of ultra-high temperature ceramic matrix composites, UHTCMCs- a review. Int Mater Rev. 2020; 65(7):389-444. https://doi.org/10.1080/09506608.2019.1652006

29. Tekin S. Sintering and densification behavior of GDC infiltrated porous GDC electrolyte. Izmir Institute of Technology; 2021.
30. Sharma N, Alam SN, Ray BC. Fundamentals of Spark Plasma Sintering (SPS): An ideal processing technique for fabrication of metal matrix nanocomposites. Spark Plasma Sintering of Materials: Advances in Processing and Applications. Springer; 2019. p. 21-59.
31. Abdullah MH. Enhancement of properties of zirconia-based ceramic composites by controlling the characteristics of reinforcement species; 2012.
32. German RM. Computer modeling of sintering processes. Int J Powder Metall. 2002; 38(2):48-66.
33. German RM. Sintering: From empirical observations to scientific principles. Butterworth-Heinemann; 2014.
34. Zawrah MF, Taha MA, Youness RA. Advanced ceramics: Stages of development. AMRT; 2023. p. 1-46.
35. Bengisu M. Production of ceramic bodies. Eng Mat. Springer; 2001. p. 85-207.
36. Sweeney SM. Permeability, drying, and sintering of pressure filtered ceramic nanopowders; 2005.
37. Myers KM. Structure-property relationship of binder jetted fused silica preforms to manufacture ceramic-metallic interpenetrating phase composites. Youngstown State University; 2016.
38. Milisavljevic I, Pitcher MJ, Li J, Chenu S, Allix M, Wu Y. Crystallization of glass materials into transparent optical ceramics. Int Mater Rev. 2023; 68(6):648-676. https://doi.org/10.1080/09506608.2022.2107372
39. Murray JW, Jin X, Cleaver CJ, Azevedo JMC, Liao Z, Zhou W, *et al*. A review of principles and options for the re-use of machining chips by solid, semi-solid or melt-based processing. J Mater Process Technol. 2024; 331:118514. https://doi.org/10.1016/j.jmatprotec.2024.118514
40. Treccani L. Processing methods for advanced ceramics. Surface-Functionalized Ceramics: For Biotechnological and Environmental Applications. Willey; 2022. https://doi.org/10.1002/9783527698042.ch2
41. Palmero P. Structural ceramic nanocomposites: A review of properties and powders synthesis methods. Nanomaterials. 2015; 5(2):656-696. https://doi.org/10.3390/nano5020656
42. Arora P. Design, manufacturing and development of hybrid manufacturing system for rapid investment casting. University of Alberta; 2024. https://doi.org/10.7939/r3-j4by-4237
43. Binner J, Hogg P, Murphy J. Advanced materials source book. 1st ed. Elsevier; 1994.
44. Lee WE, Rainforth WM. Ceramic microstructures: Property control by processing. Springer; 1994.
45. Kalin M. Aqueous lubrication of ceramics. Aqueous Lubrication. World Scientific; 2014. p. 73-101.
46. Hu ZY, Wan Y, Duan YJ, Shi YH, Gu CP, Ma R, *et al*. A review of the impact of graphene oxide on cement composites. Nanomaterials. 2025; 15(3):216. https://doi.org/10.3390/nano15030216
47. Sun Y, Li S, Zhao Q, Cong Z, Xia Y, Jiao X, *et al*. Recent advancements in alumina-based high-temperature insulating materials: Properties, applications, and future perspectives. High-Temp Mat. 2025; 2(1):10001. https://doi.org/10.70322/htm.2025.10001
48. Farooq MT, Nunthavarawong P, Mohimi A, Daopiset S. Tribo-corrosion maps of thermally sprayed cemented carbide coatings: A critical review. Surf Eng. 2025; 41(3):1-21. https://doi.org/10.1177/02670844251320066
49. Alok N, Sarath S, Jayalakshmi CG, Kandasubramanian B, Anand A, Masato D. Processing of continuous fibre-reinforced thermoplastic composites. Polymers, Materials, and Technology. Routledge Resources Online; 2025. p. 1-20. https://doi.org/10.1201/9780367694265-EPPMPT73-1